Electron Waves in the π^* Surface Band of the Si(001) Surface

Takashi Yokoyama,[1] Masakuni Okamoto,[1] and Kunio Takayanagi[1,2]
[1]*Takayanagi Particle Surface Project, ERATO, Japan Science and Technology Corporation, 3-1-2 Musashino, Akishima, Tokyo 196, Japan*
[2]*Department of Material Science and Engineering, Tokyo Institute of Technology, 4259 Nagatsuta, Midori-ku, Yokohama 227, Japan*
(Received 15 May 1998)

The unoccupied π^* surface band of the Si(001)-$c(4 \times 2)$ surface has been determined from standing-wave patterns using low-temperature scanning tunneling microscopy. A straight chain of Al ad-dimers, formed by deposition at room temperature, works as a one-dimensional (1D) barrier that scatters the surface-state electrons. The standing waves have been observed along Si dimer rows in a sample voltage range of 0.9–1.3 V at $T = 63$ K. The relationship between their wavelengths and the sample voltages gives the dispersion relation of the π^* surface band. The height and width of the potential barrier have been estimated according to the 1D Schrödinger equation. [S0031-9007(98)07398-0]

PACS numbers: 61.16.Ch, 72.10.Fk, 73.20.At

The electronic structures of material surfaces play an important role in determining the surface properties, such as chemical reactions, catalysis, and epitaxy. The surface band structures have been studied extensively with angle-resolved photoelectron spectroscopy (ARPES) and inverse photoemission spectroscopy (IPES). In recent years, scanning tunneling microscopy (STM) and spectroscopy (STS) have provided a unique opportunity to study the local electronic properties of both occupied and unoccupied surface states, with atomic resolution [1]. In addition, STM has demonstrated direct imaging of electron standing waves on metal surfaces, which result from scattering of nearly free electrons in the surface states at steps, defects, and adsorbates [2–9]. The standing waves have given important information about the dispersion relation of surface states [2–5], as well as about the electron-scattering process at a potential barrier [2,3]. In particular, it is of great interest that analysis of the standing waves has succeeded in determining surface dispersions with almost the same accuracy of ARPES or IPES methods, although these observations have been done only for the noble metal surfaces [2–5].

In this Letter, we focus on the surface states of the Si(001)-$c(4 \times 2)$ surface that is the most important surface for semiconductor devices. The $c(4 \times 2)$ reconstruction results from the antiphase ordering of buckled dimers, which is transformed to the 2×1 structure above around 200 K, due to the flip-flop motion of the buckled dimers [10]. The Si(001) surface has occupied π and unoccupied π^* surface states in the bulk band gap, both of which originate from dangling bonds of the buckled dimers. The occupied π surface bands (π_1, π_2) of the $c(4 \times 2)$ surface have been fully investigated by ARPES at $T = 120$ K [11], in accordance satisfactorily with the calculation results [12–14]. Experiments on the unoccupied π^* surface bands (π_1^*, π_2^*) of the $c(4 \times 2)$ surface have not been reported, although an IPES study for the room temperature 2×1 surface has revealed two dispersion branches that might be related to local $p(2 \times 2)$ and/or $c(4 \times 2)$ periodicities [15]. Here we report the dispersion relation of the π^* surface states of the Si(001)-$c(4 \times 2)$ surface derived from the standing-wave patterns in STM images at $T = 63$ K. A straight chain of Al dimers formed on the Si(001) surface is used as a potential barrier for the electron waves in the surface states. In unoccupied-state STM images, the standing-wave patterns have been observed in the direction parallel to the Si dimer row. The dispersion relation obtained from the sample voltage dependence of the wavelength accords well with that for the π_1^* surface band which has been theoretically derived [12–14]. In addition, by quantitatively comparing the STM data to the one-dimensional scattering model, we estimate that the Al chain works as the impenetrable hard wall potential of 0.43-nm width for the π^* state electrons.

The experiments were performed with a low-temperature STM in an ultrahigh-vacuum chamber with a base pressure less than 2×10^{-9} Pa [10]. The p-type Si(001) sample (B doped with 0.01–0.02 Ω cm) was cut from a commercial wafer stock. The sample was cleaned by flashing at 1450 K after being degassed for 20 h at 850 K, and slowly cooled to room temperature (3 K/s). A small amount of Al (about 0.05 monolayer) was deposited on the room-temperature surface from a heated tungsten filament. The sample was then transferred to the low-temperature STM stage. The STM images were acquired in a constant-current mode of 100 pA at $T = 63$ K.

Figure 1(a) shows a STM image of a sample surface at $T = 63$ K. Aluminum was arranged in a long straight line perpendicular to the dimer row of the Si(001) surface. The surface exhibits the $c(4 \times 2)$ structure, whereas the 2×1 domains have also been observed near the straight line of Al even at $T = 63$ K. Referring to the theoretical and experimental studies on the Si(001)-Al surface [16–18], the straight line in Fig. 1(a) is composed of Al

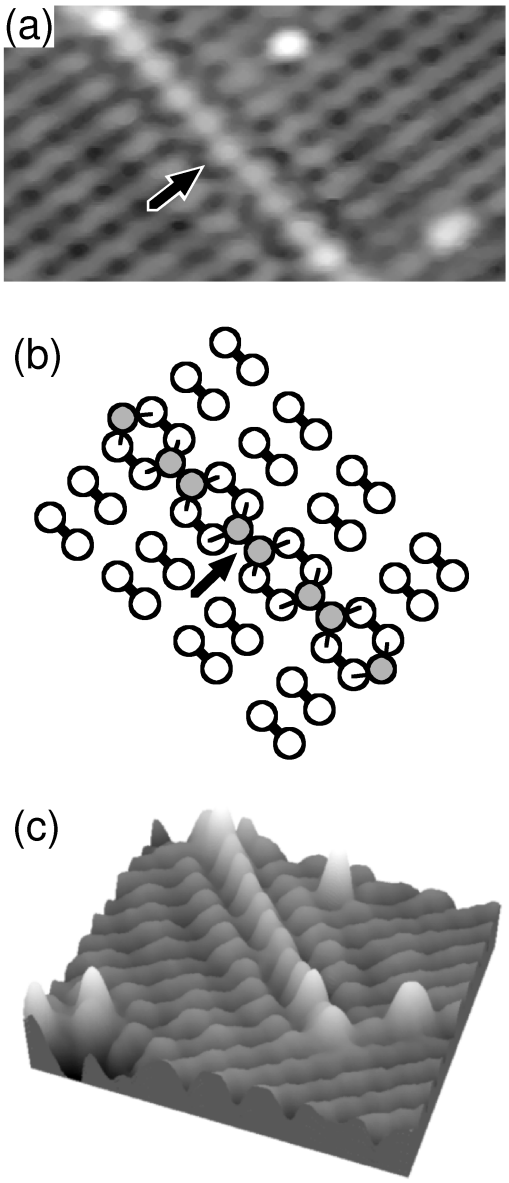

FIG. 1. (a) STM image and (b) schematic top view of a Si(001)-Al surface. The STM image extends over 11.3 × 6.2 nm^2 taken at $T = 63$ K and $V_s = 1.2$ V. The Al ad-dimers are arranged in a straight line perpendicular to the Si dimer row, whereas the Al ad-dimers run parallel to the underlying Si-Si dimer bonds. As denoted by arrows in (a) and (b), the bright protrusion in the Al chain corresponds to an Al ad-dimer located between the Si dimer rows. (c) The perspective view of the STM image at $V_s = 1.2$ V. The straight Al chain exists at the center of the image. Standing-wave patterns along the Si dimer rows are shown on the left- and right-hand sides of the Al chain. The dominant peaks appear periodic, with a spacing of 1.8 nm, and are damped away from the Al chain.

ad-dimers, as schematically shown in Fig. 1(b). In the unoccupied STM image, the bright protrusion corresponds to an Al ad-dimer, located between Si dimer rows without the disruption of the underlying Si-Si dimer bonds. This model suggests that the Al ad-dimer strongly interacts with the dangling-bond states of the underlying Si dimers to form local bonds. The interaction breaks the surface-state bands for electrons propagating in the dimer-row direction. Thus, the straight chain of the Al ad-dimers may act as a one-dimensional (1D) potential barrier for the electrons in the occupied and/or unoccupied surface bands. The Al dimer chain scatters the surface-state electrons, and the quantum interference between the incoming and outgoing electron waves results in the standing-wave formation on the Si(001)-$c(4 \times 2)$ surface.

Figure 1(c) shows the perspective view of the STM image at $V_s = 1.2$ V. On the left- and right-hand sides of the Al dimer chain, the spatial oscillations are shown in the direction of the Si dimer row. The oscillation is uniform in the direction parallel to the Al dimer chain, while it is damped away from the chain. Although the oscillation is not simple sinusoidal, the dominant peaks appear periodic, with a spacing of 1.8 nm. Similar oscillations were observed in a bias voltage range of 0.9–1.3 V, and disappeared above 1.4 V. Figure 2 shows the cross sections of the spatial oscillations at different bias voltages. The oscillation periods became shorter with increasing bias voltage.

The spatial oscillations result from the scattering of the surface-state electrons at the Al dimer chain. The surface states of the Si(001)-$c(4 \times 2)$ surface exhibit 1D character along the dimer row (the Γ-J' line in the surface Brillouin zone). Although the correlation for dimer buckling between dimer rows results in the

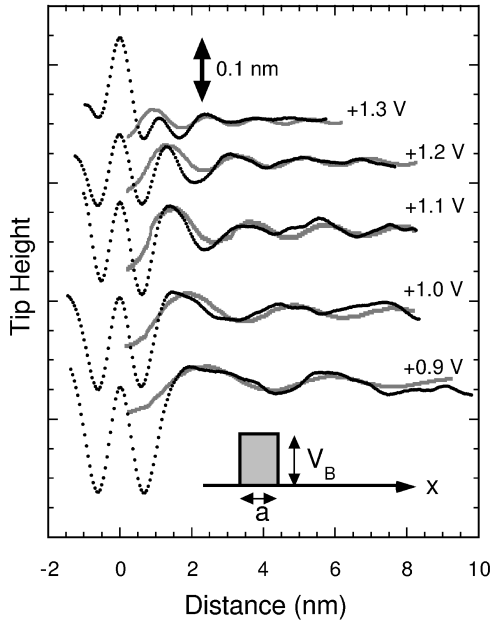

FIG. 2. Cross sections of the standing-wave patterns along the Si dimer rows at sample bias voltages from 0.9–1.3 V. The curves have been shifted vertically for viewing. On the left-hand side, the first peaks correspond to the Al chain. Gray line: Calculated z oscillations using Eqs. (2) and (3). Inset: Schematic view of the one-dimensional square potential model for the electron scattering. In this model, the Al chain works as the square potential of width a and height V_B.

$c(4 \times 2)$ reconstruction, the interaction energy has been calculated to be only about 2 meV/dimer [12]. Because of the weak correlation, the nearly flat dispersion for direction perpendicular to the dimer row (the Γ-J line) has been obtained from the calculations for the Si(001)-$c(4 \times 2)$ surface [12,13]. In the surface states, therefore, the electron waves propagate only in the direction of the Si dimer row. Moreover, the straight Al chain running perpendicular to the Si dimer row works as the 1D potential barrier. These results exclude the influence of the scattered and propagated electron waves in the direction perpendicular to the dimer row. Thus, one can analyze the standing-wave patterns as the 1D quantum interference in the dimer-row direction. For simplicity, we modeled the Al dimer chain as a square potential barrier of width a and height V_B, as schematically shown in the inset of Fig. 2. Provided that the center of the Al chain is located at $x = 0$, a 1D Bloch wave along the dimer rows (x direction) encounters the potential barrier at $x = a/2$. The wave function of the standing wave is described as $\psi(k, x) = e^{-ikx} + Re^{i(kx+\delta)}$, leading to a spatial oscillation in the local density of states (LDOS) at the energy relative to the Fermi level $E(k) = eV_s$:

$$|\psi(k, x)|^2 = 1 + R^2 + 2R\cos(2kx + \delta), \qquad (1)$$

where R is the reflection coefficient, and δ is the phase shift. If the density of states of the STM tip is assumed to be constant, the tunneling current I_t at the sample voltage V_s is given by

$$I_t \propto \int_0^{eV_s} T(E, eV_s, z)\,|\psi(k, x)|^2 dE = \int_0^{eV_s} T(E, eV_s, z)\{1 + R^2 + 2R\cos(2kx + \delta)\}dE, \qquad (2)$$

where $T(E, eV_s, z)$ is the tunneling probability, and z is the distance between the tip and sample surface. According to Eq. (2), the constant-current images are generated by the weighted integral of the LDOS maps. Because of the maximum tunneling probability $T(eV_s, eV_s, z)$ at $E = eV_s$, the LDOS at $E = eV_s$ strongly contributes to the tunneling current I_t. This leads to a significant enhancement of the spatial LDOS oscillation at $E = eV_s$ in the constant-current z oscillation, although the z oscillation is not proportional to the spatial LDOS oscillation. If the periodic spacing λ_z of the z oscillation almost corresponds to the wavelength λ_ρ of the spatial LDOS oscillation at $E = eV_s$ [19], the wave number k of the LDOS oscillation can be estimated as $k = \pi/\lambda_z$. According to this approximation, we plot an energy dispersion of the standing waves from a series of the z oscillations in Fig. 2. Figure 3 shows the dispersion curve in the Γ-$\frac{1}{2}J'$ line of the surface Brillouin zone. This result is in good agreement with previous calculations for the π_1^* surface states [12–14]. In Fig. 3, our obtained

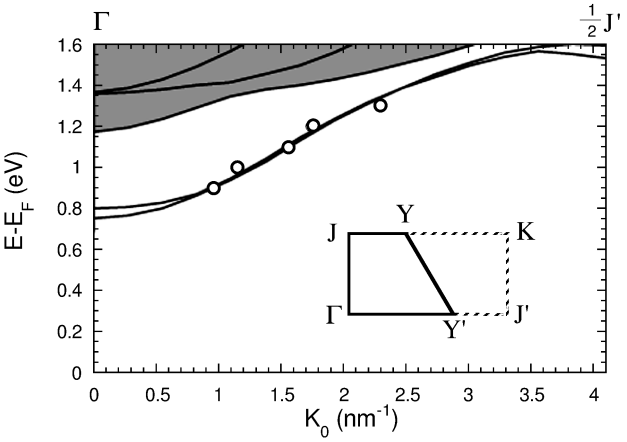

FIG. 3. Dispersion relation of the π^* surface states along the Γ-$\frac{1}{2}J'$ line (the dimer-row direction), obtained from the standing waves. Solid line: Calculated band structure of the Si(001)-$c(4 \times 2)$ surface in the Γ-$\frac{1}{2}J'$ line from Ref. [12]. The LDA calculations systematically underestimate band gaps, so that the calculation bands have been shifted upwards in energy by 0.65 eV. Shaded area represents the projected bulk bands. Inset: Surface Brillouin zones of the $c(4 \times 2)$ and 2×1 structures denoted by solid and dotted lines, respectively.

dispersions are superimposed on the calculated bands of the Si(001)-$c(4 \times 2)$ surface by Ramstad *et al.* using the local-density approximation (LDA) [12]. The calculated bands have been shifted upwards in energy by 0.65 eV, because first the LDA calculations systematically underestimate band gaps, and second the Fermi level position should be shifted for our highly doped p-type sample. Johansson and Reihl [15] have reported a similar dispersion curve for the room-temperature Si(001)-2×1 surface in the Γ-$\frac{1}{2}J'$ line by IPES [15]. In the IPES study, two dispersion branches indicate local $p(2 \times 2)$ and/or $c(4 \times 2)$ periodicities, although the 2×1 symmetry dominates on the room-temperature Si(001) surface. The dispersion relation of the $c(4 \times 2)$ surface in Fig. 3, on the other hand, is about 0.3–0.4 eV higher than the IPES dispersion. This energy shift results from the difference between n- and p-type samples; the shift of the Fermi level positions by dopants. The surface photovoltage study [20] has determined the Fermi level shift to be 0.3–0.4 eV for a p-type Si(001) surface, compared to an n-type one at $T = 85$ K. We examined the energy shift between p- and n-type surfaces (0.01–0.02 Ω cm and 0.05–0.09 Ω cm, respectively) using STS at $T = 63$ K. The relative energy shift of 0.3–0.35 eV in the STS spectra (not shown) accords well with the photovoltage experiment and also with the IPES experiment.

Although the dispersion relation of the π^* states can be obtained from the constant-current STM data, the phase and shape of the z oscillation differ from those of the spatial LDOS oscillation [4]. To clarify the scattering phenomena of the π^* state electrons, we calculated

the constant-current z oscillations using the dispersion relation and Eq. (2). Although the energy dependence of the tunneling probability $T(E, eV_s, z)$ is not clear at present, it is given by the WKB approximation as [1]

$$T(E, eV_s, z) = \exp\left\{-2z\sqrt{\frac{2m}{\hbar^2}\left(\bar{\phi} + \frac{eV_s}{2} - E\right)}\right\}, \quad (3)$$

where $\bar{\phi} \approx 4.5eV$ is the average work function of the tip and sample surface. In Eq. (2), the phase shift δ of the LDOS oscillation at $E = eV_s$ is obtained from the 1D Schrödinger equation as a function of a and V_B. From the result of the calculation, the simulated z oscillations, using $V_B =$ infinity and $a = 0.43$ nm, well reproduced the STM data, as shown in Fig. 2. The values of V_B and a were changed little, even for the tunneling probability $T = \exp[-2z\sqrt{(2m/\hbar^2)\bar{\phi}}]$. This result suggests that the energy dependence of $T(E, eV_s, z)$ does not strongly affect the barrier height and width of the Al chain in this energy range.

In occupied-state STM images, the spatial oscillation was not observed in spite of the existence of the π surface states. The theoretical [12,13] and ARPES [11] results have revealed that the π surface state lies close to the bulk band edge along the Γ-J' line. Although the reason for the no standing waves in the occupied-state images is unknown, the connection between the π states and the bulk states suggests that most of the π state electrons can be scattered into the bulk bands, leading to strong damping of the standing waves.

For the unoccupied π^* state electrons, the impenetrable hard wall potential is generated by the break of the surface bands at the Al ad-dimer chain, which indicates the existence of the energy gap at the Al-Si(001) interface. Similar standing waves were also observed at the lower side of the S_A steps, but the oscillation amplitude was only about $1/5$ of that near the Al dimer chain. Furthermore, in spite of the break of the surface bands, we could not observe the standing waves both at the upper side of the S_B steps and near missing-dimer defects. These results indicate that the electronic structure of the local bonds at adsorbates, steps, and defects seems to determine the effective barrier height, as well as the transmission probability to the bulk states. By using other materials for the potential barrier, the standing-wave studies will provide detailed information about the local bond nature of the metal- or semiconductor-Si(001) interfaces.

In summary, using the low-temperature STM, we have observed the standing waves generated by the scattering of the electrons in the π^* surface states on the Si(001)-$c(4 \times 2)$ surface. Based on the 1D square potential model, the surface dispersion of the π^* states has been obtained from the STM data. In addition, the Al dimer chain has been found to act as an impenetrable hard wall of 0.43-nm width for the electrons in the π^* surface band.

We thank Dr. A. Ramstad and Dr. G. Brocks for sending their calculation data [12] in Fig. 3.

[1] For example, R. J. Hammers, Annu. Rev. Phys. Chem. **40**, 531 (1989); R. M. Feenstra, Surf. Sci. **299/300**, 965 (1994).
[2] M. F. Crommie, C. P. Lutz, and D. M. Eigler, Nature (London) **363**, 524 (1993); Science **262**, 218 (1993); E. J. Heller, M. F. Crommie, C. P. Lutz, and D. M. Eigler, Nature (London) **369**, 464 (1994).
[3] Y. Hasegawa and Ph. Avouris, Phys. Rev. Lett. **71**, 1071 (1993); Ph. Avouris, I.-W. Lyo, R. E. Walkup, and Y. Hasegawa, J. Vac. Sci. Technol. B **12**, 1447 (1994); Ph. Avouris and I.-W. Lyo, Science **264**, 942 (1994).
[4] J. Li, W. Schneider, and R. Berndt, Phys. Rev. B **56**, 7656 (1997).
[5] W. Chen, V. Madhavan, T. Jamneala, and M. F. Crommie, Phys. Rev. Lett. **80**, 1469 (1998).
[6] J. Li, W. Schneider, R. Berndt, and S. Crampin, Phys. Rev. Lett. **80**, 3332 (1998).
[7] P. T. Sprunger *et al.*, Science **275**, 1764 (1997).
[8] Ph. Hofmann *et al.*, Phys. Rev. Lett. **79**, 265 (1997).
[9] D. Fujita *et al.*, Phys. Rev. Lett. **78**, 3904 (1997).
[10] T. Yokoyama and K. Takayanagi, Phys. Rev. B **56**, 10 483 (1997); Phys. Rev. B **57**, R4226 (1998).
[11] Y. Enta, S. Suzuki, and S. Kono, Phys. Rev. Lett. **65**, 2704 (1990).
[12] A. Ramstad, G. Brocks, and P. J. Kelly, Phys. Rev. B **51**, 14 504 (1995).
[13] Z. Zhu, N. Shima, and M. Tsukada, Phys. Rev. B **40**, 11 868 (1989).
[14] J. E. Northrup, Phys. Rev. B **47**, 10 032 (1993).
[15] L. S. O. Johansson and B. Reihl, Surf. Sci. **269/270**, 810 (1992).
[16] J. Nogami, A. A. Baski, and C. F. Quate, Phys. Rev. B **44**, 1415 (1991).
[17] H. Itoh, J. Itoh, A. Schmid, and T. Ichinokawa, Phys. Rev. B **48**, 14 663 (1993).
[18] G. Brocks, P. J. Kelly, and R. Car, Phys. Rev. Lett. **70**, 2786 (1993).
[19] For the Ag(111) surface, Schneider *et al.* have revealed that the periodic spacing λ_z of the z oscillation almost corresponds to the λ_ρ at $E = eV_s$ in Ref. [4].
[20] W. Mönch, P. Koke, and S. Krueger, J. Vac. Sci. Technol. **19**, 313 (1981).